

Determination of thermodynamic parameters of nanocalcium molybdate reaction system by microcalorimetry

Gaochao Fan, Zaiyin Huang

College of Chemistry & Ecological Engineering, Guangxi University for Nationalities, Nanning 530006, People's Republic of China
E-mail: hzy210@163.com

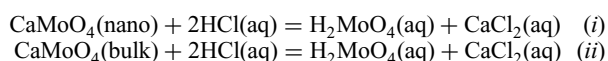
Published in Micro & Nano Letters; Received on 9th July 2013; Revised on 7th August 2013; Accepted on 19th August 2013

Calcium molybdate (CaMoO_4) nanorods with uniform size were harvested by a gentle and facile reverse-microemulsion method. Each of the prepared nanorods was about 250 nm in length and 80 nm in diameter. By combining thermodynamic and thermokinetic theories, thermodynamic parameters of the nano CaMoO_4 reaction system such as standard molar enthalpy of reaction ($\Delta_r H_m^\theta$), standard molar activation Gibbs free energy of reaction ($\Delta_r^\ddagger G_m^\theta$), standard molar activation enthalpy of reaction ($\Delta_r^\ddagger H_m^\theta$) and standard molar activation entropy of reaction ($\Delta_r^\ddagger S_m^\theta$) were successfully acquired by applying microcalorimetry. The significant differences of the thermodynamic parameters between nano CaMoO_4 and bulk CaMoO_4 reaction systems are also discussed and the reason can be rooted in the surface effect of nanomaterials.

1. Introduction: Calcium molybdate (CaMoO_4) with a scheelite type has attracted intense interest thanks to its potential application in various fields such as photoluminescence [1, 2], scintillation detectors [3, 4], catalysts [5], optical fibres [6], energy storage [7], microwave applications [8] and so on. It is well known that nanostructured materials have many special and interesting properties which are different from their bulks. For this reason, a variety of strategies have been reported to prepare CaMoO_4 nanoscale structures with different sizes and morphologies [9–15]. Currently, many properties of CaMoO_4 nanoscale structures have been well studied, however to the best of our knowledge very few thermodynamic properties are available.

The thermodynamic property of the nanoreaction system is an expression for the thermodynamic property of nanomaterials [16, 17]. It is an important research target for nanoreaction thermodynamics to gain thermodynamic parameters, explore the variation of thermodynamic parameters with size and morphology and establish a theoretical model for the nanoreaction system [18]. In addition, the data of thermodynamic parameters plays an important role in the theoretical study, application development and industrial production of compounds. In this Letter, we present a gentle and facile route for preparing CaMoO_4 nanorods with uniform size, and an effective and general route for obtaining thermodynamic parameters of nanomaterial reaction systems by microcalorimetry.

2. Methodology: The reaction systems studied in this reported work are listed as follows



A RD496-III type microcalorimeter, based on thermokinetic theory, can provide both thermodynamic and kinetic information at the same time. The thermokinetic equation for irreversible reactions at constant temperature and pressure is as follows [19]

$$\ln \left[\frac{1}{H_\infty} \frac{dH_i}{dt} \right] = \ln k + n \ln \left[1 - \frac{H_i}{H_\infty} \right] \quad (1)$$

where H_∞ is the total enthalpy of a reaction, k is the rate constant represented with conversion and its unit is s^{-1} , n is the reaction order and (dH_i/dt) the enthalpy change rate. Hence, the rate

constant (k) can be obtained through regression analysis of the thermokinetic data.

In the present calorimetric experiment, each reaction occurred at temperatures of 298.15 K (defined as T_1) and 303.15 K (defined as T_2), respectively. Applying (1), the corresponding rate constants of k_1 and k_2 can be obtained.

According to the following relationship between the rate constant and standard molar activation Gibbs free energy of reaction [20], the standard molar activation Gibbs free energies of reactions $\Delta_r^\ddagger G_m^\theta(1)$ and $\Delta_r^\ddagger G_m^\theta(2)$ for the reaction temperatures T_1 and T_2 can be obtained

$$k = \frac{k_B T}{h} \exp \left(\frac{-\Delta_r^\ddagger G_m^\theta}{RT} \right) \quad (2)$$

where k_B and h represent the Boltzmann and Planck constant, respectively.

Then, combining (2) with the following fundamental equation of thermodynamics, the standard molar activation enthalpy of reaction $\Delta_r^\ddagger H_m^\theta(1)$ and $\Delta_r^\ddagger H_m^\theta(2)$, and the standard molar activation entropy of reaction $\Delta_r^\ddagger S_m^\theta(1)$ and $\Delta_r^\ddagger S_m^\theta(2)$ can be achieved

$$\Delta_r^\ddagger G_m^\theta = \Delta_r^\ddagger H_m^\theta - T \Delta_r^\ddagger S_m^\theta \quad (3)$$

Thus, the thermodynamic parameters of $\Delta_r H_m^\theta$, $\Delta_r^\ddagger G_m^\theta$, $\Delta_r^\ddagger H_m^\theta$ and $\Delta_r^\ddagger S_m^\theta$ can be acquired from the above methodology.

3. Experimental: Bulk CaMoO_4 (particle size is up to a dozen or even dozens of micrometres) with purity higher than 99.98% was purchased from the Alfa Aesar Chemicals Company. Calcium chloride (CaCl_2), sodium molybdate ($\text{Na}_2\text{MoO}_4 \cdot 2\text{H}_2\text{O}$), TritonX-100 (OP), *n*-octanol, cyclohexane and hydrochloric acid were purchased from the Xilong Chemical Reagent Factory. All the reagents employed in the present work were of analytical grade. The experimental procedure included two steps: (i) synthesis and characterisation of CaMoO_4 nanorods; and (ii) reaction calorimetry on both the nano CaMoO_4 and bulk CaMoO_4 reaction systems.

A typical synthesis process for the CaMoO_4 nanorods is as follows: two microemulsion solutions were prepared by adding 1.32 ml of 0.01 M Na_2MoO_4 and 1.32 ml of 0.01 M CaCl_2

aqueous solution into a 13 ml TritonX-100/*n*-octanol/cyclohexane system (according to the volume ratio 3/2/8), respectively. After 10 min of vigorous stirring, the two microemulsion solutions were mixed slowly and stirred for another 20 min. The resulting solution was aged without stirring for 48 h at room temperature. The white precipitates were separated by centrifugation, washed with acetone, deionised water and absolute ethanol and then dried in a vacuum at room temperature. Finally, the as-synthesised products were harvested.

Reaction calorimetry was conducted by a microcalorimeter (RD496-III, Mianyang CP Thermal Analysis Instrument Co. Ltd). The microcalorimeter was calibrated by Joule effect and its calorimetric constant was $(63.205 \pm 0.031) \mu\text{V} \cdot \text{mW}^{-1}$ at the experimental temperature of 298.15 K. The dissolution enthalpy of KCl in deionised water was measured to be $(17.469 \pm 0.036) \text{kJ} \cdot \text{mol}^{-1}$, which was in good agreement with the value of $(17.524 \pm 0.028) \text{kJ} \cdot \text{mol}^{-1}$ in [21]. This indicates that the calorimetric system is accurate and reliable. Reaction calorimetry on both the nanoCaMoO₄ and bulk CaMoO₄ reaction systems was conducted at the experimental temperature of 298.15 and 303.15 K, respectively. The CaMoO₄ (nano or bulk) and HCl solution were placed in a stainless steel sample cell in separate 15 ml containers [22]. 1.0 ml of 1.0 M HCl solution was placed in a small glass tube above the 1.269 mg CaMoO₄, which was in a larger glass tube. After establishment of equilibrium, the small glass tube with HCl solution was pushed down simultaneously. This led the HCl and CaMoO₄ to react with each other, and the in situ thermodynamic and kinetic information for the reaction process was recorded by the microcalorimeter.

4. Results and discussion: The typical X-ray diffraction (XRD) pattern of the as-synthesised products is shown in Fig. 1a. All the diffraction peaks of the products can be indexed to the pure tetragonal phase of CaMoO₄ with the cell parameters of $a = 5.19 \text{ \AA}$ and $c = 11.25 \text{ \AA}$ (JCPDS Card No. 029-0351). No impurity peaks were detected, indicating the formation of pure products. The sharp and narrow diffraction peaks suggest that the prepared products are highly crystallised. Fig. 1b represents the SEM image of the prepared products. The SEM image reveals that a large number of CaMoO₄ nanorods with uniform size have been achieved. Each rod was about 250 nm in length and 80 nm in diameter.

Fig. 2 displays a typical in situ microcalorimetric heat flow curve of the reaction between CaMoO₄ nanorods and HCl solution. Figs. 2a and b are related to the reaction temperature of 298.15 and 303.15 K, respectively. H_{∞} can be obtained by integrating the area enclosed by the heat flow curve and basis line. Combined with the amount of CaMoO₄ nanorods, standard molar enthalpy of reaction $\Delta_r H_m^{\theta}(1) = -107.48 \text{ kJ} \cdot \text{mol}^{-1}$ and $\Delta_r H_m^{\theta}(2) = -95.23 \text{ kJ} \cdot \text{mol}^{-1}$ are calculated. Applying (1), $k_1 =$

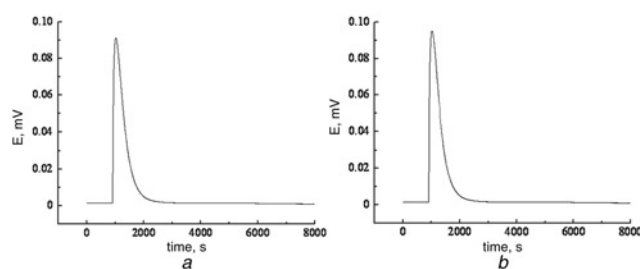


Figure 2 In situ microcalorimetric heat flow curve of the reaction between CaMoO₄ nanorods and HCl solution at temperatures of 298.15 and 303.15 K
a 298.15 K
b 303.15 K

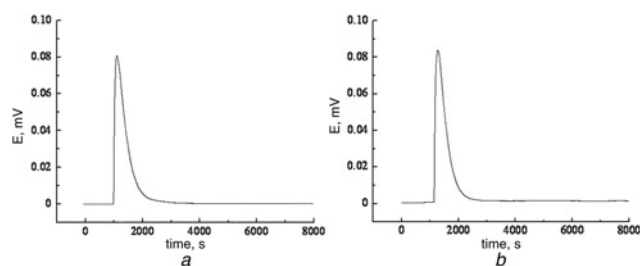


Figure 3 In situ microcalorimetric heat flow curve of the reaction between bulk CaMoO₄ and HCl solution at temperatures of 298.15 and 303.15 K
a 298.15 K
b 303.15 K

$1.907 \times 10^{-3} \text{ s}^{-1}$ and $k_2 = 2.241 \times 10^{-3} \text{ s}^{-1}$ are obtained through regression analysis of the thermokinetic data recorded by the microcalorimeter. Then, employing (2), $\Delta_r^{\#} G_m^{\theta}(1) = 88.56 \text{ kJ} \cdot \text{mol}^{-1}$ and $\Delta_r^{\#} G_m^{\theta}(2) = 89.67 \text{ kJ} \cdot \text{mol}^{-1}$ are obtained. Subsequently, according to (3), $\Delta_r^{\#} H_m^{\theta}(2) = 22.37 \text{ kJ} \cdot \text{mol}^{-1}$ and $\Delta_r^{\#} S_m^{\theta} = -222.00 \text{ J} \cdot \text{mol}^{-1} \cdot \text{K}^{-1}$ are obtained combined with both the values of $\Delta_r^{\#} G_m^{\theta}(1)$ and $\Delta_r^{\#} G_m^{\theta}(2)$.

Fig. 3 exhibits a typical in situ microcalorimetric heat flow curve of the reaction between bulk CaMoO₄ and HCl solution. Figs. 3a and b are related to the reaction temperature of 298.15 and 303.15 K, respectively. In the same way, the thermodynamic parameters of $\Delta_r H_m^{\theta}$, $\Delta_r^{\#} G_m^{\theta}$, $\Delta_r^{\#} H_m^{\theta}$ and $\Delta_r^{\#} S_m^{\theta}$ for the bulk CaMoO₄ reaction system are obtained.

Reaction calorimetry for each reaction system at each temperature was conducted five times. For comparison purposes, the thermodynamic parameters at 298.15 K for each reaction system are displayed in Table 1.

It is worth noting that significant differences of thermodynamic parameters exist between the nanoCaMoO₄ and bulk CaMoO₄

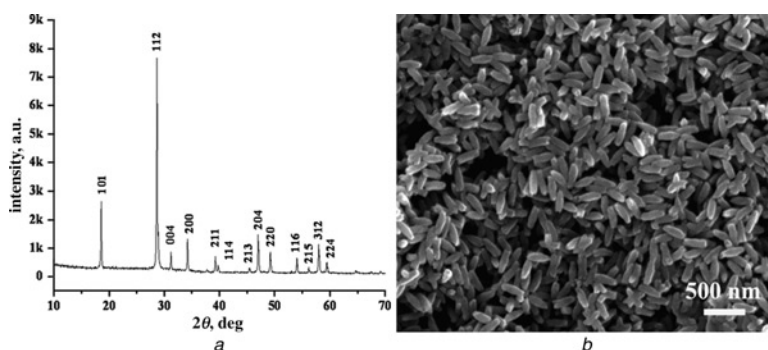


Figure 1 Typical XRD pattern and SEM image of the prepared CaMoO₄ nanorods
a Typical XRD pattern
b SEM image

Table 1 Thermodynamic parameters at 298.15 K of CaMoO₄ reaction systems

Reaction system	No.	$\Delta_r H_m^\theta$, kJ · mol ⁻¹	$\Delta_r^\# G_m^\theta$, kJ · mol ⁻¹	$\Delta_r^\# H_m^\theta$, kJ · mol ⁻¹	$\Delta_r^\# S_m^\theta$, kJ · mol ⁻¹
bulk CaMoO ₄	1	-67.66	90.73	61.51	-98.00
	2	-67.54	90.65	61.46	-97.90
	3	-67.62	90.78	61.54	-98.07
	4	-67.68	90.70	61.49	-97.97
	5	-67.73	90.68	61.55	-97.70
average value		-67.65	90.71	61.51	-97.94
nano CaMoO ₄	1	-107.48	88.56	22.37	-222.00
	2	-107.54	88.67	22.45	-222.14
	3	-107.50	88.52	22.42	-221.70
	4	-107.43	88.55	22.34	-222.07
	5	-107.48	88.63	22.48	-221.87
average value		-107.49	88.59	22.41	-221.97

reaction systems. Compared with the bulk CaMoO₄ reaction system, the values of the thermodynamic parameters ($\Delta_r H_m^\theta$, $\Delta_r^\# G_m^\theta$, $\Delta_r^\# H_m^\theta$ and $\Delta_r^\# S_m^\theta$) for the nanoCaMoO₄ reaction system are obviously small. According to our previous literature [16–18], the nanoCaMoO₄ and bulk CaMoO₄ reaction systems possess the same final state and transition state, and the only difference is the initial state. Owing to nanometre size, the surface effect of nanoCaMoO₄ causes the metastable state of the nanoreaction system. Combined with the characteristics of the state function, the values of the thermodynamic parameters ($\Delta_r H_m^\theta$, $\Delta_r^\# G_m^\theta$, $\Delta_r^\# H_m^\theta$ and $\Delta_r^\# S_m^\theta$) for the nanoreaction system decrease, compared with its corresponding bulk reaction system. In short, the evident differences of the thermodynamic parameters between the nanoCaMoO₄ and bulk CaMoO₄ reaction systems can be attributed to the surface effect of the nanomaterials. To demonstrate, the specific surface areas of nanoCaMoO₄ and bulk CaMoO₄ were tested. The specific surface area of nanoCaMoO₄ is about 18.7853 m² · g⁻¹, whereas the specific surface area of the bulk CaMoO₄ is 0.2226 m² · g⁻¹.

5. Conclusion: In summary, CaMoO₄ nanorods with uniform size were achieved by a gentle and facile reverse-microemulsion method. Combined with the thermodynamic and thermokinetic theories, the thermodynamic parameters of $\Delta_r H_m^\theta$, $\Delta_r^\# G_m^\theta$, $\Delta_r^\# H_m^\theta$ and $\Delta_r^\# S_m^\theta$ were successfully acquired by applying microcalorimetry. The significant differences of the thermodynamic parameters between nanoCaMoO₄ and bulk CaMoO₄ reaction systems can be attributed to the surface effect of nanomaterials. Moreover, it is an effective and general route for obtaining the thermodynamic parameters of nanomaterial reaction systems.

6. Acknowledgments: This work is financially supported by the National Natural Science Foundation of China (nos 20963001 and 21273050), and the Guangxi Natural Science Foundation of China (nos 0991001z and 0991085).

7 References

- [1] Cui C.H., Bi J., Gao D.J.: 'Room-temperature synthesis of crystallized luminescent CaMoO₄ film by a simple chemical method', *Appl. Surf. Sci.*, 2008, **255**, pp. 3463–3465
- [2] Zakharko Y., Luchechko A., Syvorotka I., Stryganyuk G., Solskii I.: 'Anisotropy of optical absorption and luminescent properties of CaMoO₄', *Radiat. Meas.*, 2010, **45**, pp. 429–431
- [3] Kwan S., Kim F., Akana J., Yang P.D.: 'Synthesis and assembly of BaWO₄ nanorods', *Chem. Commun.*, 2001, **5**, pp. 447–448
- [4] Mikhailik V.B., Kraus H.: 'Cryogenic scintillators in searches for extremely rare events', *J. Phys. D, Appl. Phys.*, 2006, **39**, pp. 1181–1191
- [5] Sen A., Pramanik P.: 'Low-temperature synthesis of nano-sized metal molybdate powders', *Mater. Lett.*, 2001, **50**, pp. 287–294
- [6] Tanaka K., Miyajima T., Shirai N., Zhang Q., Nakata R.: 'Laser photochemical ablation of CdWO₄ studied with the time-of-flight mass spectrometric technique', *J. Appl. Phys.*, 1995, **77**, pp. 6581–6587
- [7] Sharma N., Shaju K.M., Rao G.V.S., Chowdari B.V.R., Dong Z.L., White T.J.: 'Carbon-coated nanophase CaMoO₄ as anode material for Li ion batteries', *Chem. Mater.*, 2004, **16**, pp. 504–512
- [8] Choi G.K., Cho S.Y., An J.S., Hong K.S.: 'Microwave dielectric properties and sintering behaviors of scheelite compound CaMoO₄', *J. Eur. Ceram. Soc.*, 2006, **26**, pp. 2011–2015
- [9] Ryu J.H., Yoon J.W., Lim C.S., Oh W.C., Shim K.B.: 'Microwave-assisted synthesis of CaMoO₄ nano-powders by a citrate complex method and its photoluminescence property', *J. Alloys Compd.*, 2005, **390**, pp. 245–249
- [10] Luo Y.S., Dai X.J., Zhang W.D., Yang Y., Sun C.Q., Fu S.Y.: 'Controllable synthesis and luminescent properties of novel erythrocyte-like CaMoO₄ hierarchical nanostructures via a simple surfactant-free hydrothermal route', *Dalton Trans.*, 2010, **39**, pp. 2226–2231
- [11] Yin Y.K., Gao Y., Sun Y.Z., *ET AL.*: 'Synthesis and photoluminescent properties of CaMoO₄ nanostructures at room temperature', *Mater. Lett.*, 2010, **64**, pp. 602–604
- [12] Ryu J.H., Choi B.G., Yoon J.W., Shim K.B., Machi K., Hamada K.J.: 'Synthesis of CaMoO₄ nanoparticles by pulsed laser ablation in de-ionized water and optical properties', *J. Lumin.*, 2007, **124**, pp. 67–70
- [13] Sun Y., Ma J.F., Jiang X.H., *ET AL.*: 'Ethylene glycol-assisted electrochemical synthesis of CaMoO₄ crystallites with different morphology and their luminescent properties', *Solid State Sci.*, 2010, **12**, pp. 1283–1286
- [14] Yu P., Hu G.B., Tian Y.F., Xiao D.Q., Liu Y., Guo Q.W.: 'Synthesis and photoluminescent properties of nanocrystalline CaMoO₄ thin film via chemical solution processing', *J. Nanosci. Nanotechnol.*, 2008, **8**, pp. 2651–2654
- [15] Gao D.J., Lai X., Cui C.H., Cheng P., Bi J., Lin D.M.: 'Oxidant-assisted preparation of CaMoO₄ thin film using an irreversible galvanic cell method', *Thin Solid Films*, 2010, **518**, pp. 3151–3155
- [16] Fan G.C., Sun L., Huang Z.Y., Jiang J.Y., Li Y.F.: 'Thermodynamic functions of the grain-like ZnO nanostructures', *Mater. Lett.*, 2011, **65**, pp. 2783–2785
- [17] Fan G.C., Jiang J.Y., Li Y.F., Huang Z.Y.: 'Thermodynamic functions of the ZnO nanowires', *Mater. Chem. Phys.*, 2011, **130**, pp. 839–842
- [18] Fan G.C., Huang Z.Y., Wang T.H.: 'Size effect on thermodynamic properties of CaMoO₄ micro/nano materials and reaction systems', *Solid State Sci.*, 2013, **16**, pp. 121–124
- [19] Gao S.L., Chen S.P., Hu R.Z., Li H.Y., Shi Q.Z.: 'Derivation and application of thermodynamic equations', *Chin. J. Inorg. Chem.*, 2002, **18**, pp. 362–366
- [20] Fu X.C., Shen W.X., Yao T.Y., Hou W.H.: 'Physical chemistry' (Higher Education Press, Beijing, 2006, 5th edn)
- [21] Rychlý R., Pekárek V.: 'The use of potassium chloride and tris (hydroxymethyl)aminomethane as standard substances for solution calorimetry', *J. Chem. Thermodyn.*, 1977, **9**, pp. 391–396
- [22] Li Y.F., Jiang J.Y., Fan G.C., Ma Y.J., Huang Z.Y.: 'Kinetic investigation of in situ growth of CdMoO₄ nano-octahedra', *Chin. Sci. Bull.*, 2011, **56**, pp. 269–274